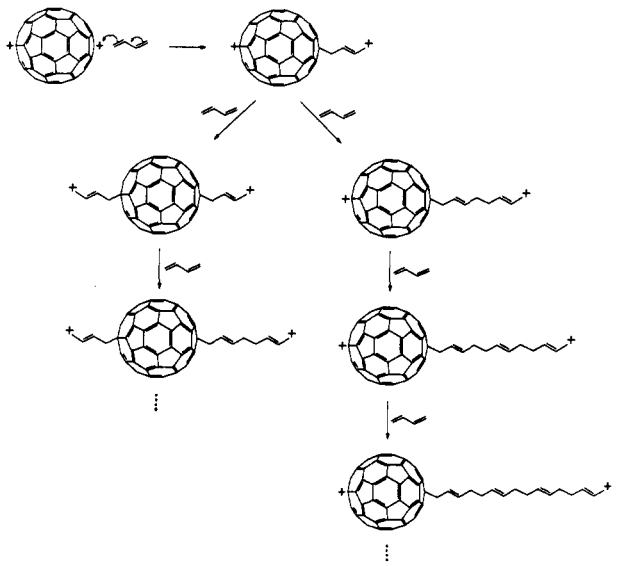

Figure 2. Proposed mechanism for the polymerization of 1,3-butadiene initiated by C_{60}^{2+}.

tadiene was also observed, but its formation proceeded at a much slower rate. The formation of the dimer ion has been noted previously in an ICR study, and collision-activated decomposition experiments with a tandem mass spectrometer have indicated that an acyclic branched chain structure is preferred at high pressures.[8] We have also observed that C_{70}^{2+} reacts with C_4H_6 in a manner which is analogous to that of C_{60}^{2+}. This is not surprising given the structural similarity of C_{60}^{2+} and C_{70}^{2+}. However, because of lower ion signals (C_{70} constitutes only a small portion (2–12%) of the fullerene mixture used in the ion source), association products of C_{70}^{2+} with C_4H_6 were observed only up to $C_{70}(C_4H_6)_3^{2+}$.

With regard to the mechanism of reaction 2, we propose that the initiation step involves addition of butadiene to C_{60}^{2+} by C–C covalent bond formation with the concomitant propagation of one of the two positive charges on the fullerene cage to a distance of four carbon atoms away from the fullerene surface to the terminal carbon of butadiene. Although this appears counterintuitive because a charge becomes less delocalized, via. delocalization energy is lost, the energy gained by the Coulombic repulsion between the two positive charges should favor the bond formation described. The Coulombic repulsion between the two positive charges will be relaxed further as more butadiene monomers are added. Two ways in which a polymer chain can be propagated, viz. on one side of the cage, in a tadpole-like fashion, or on both the sides, in a spindle-like fashion, are shown in Figure 2. Sequential addition by direct bonding to the π-system of the fullerene cage cannot be ruled out, but appears less favorable since it does not involve Coulombic relaxation and since we have found that $C_{60}^{\bullet+}$ does not react with 1,3-butadiene. It appears, therefore, that the fullerene cage may become a pendant on, or be blocked in, the polybutadiene chain. The electrostatic driving force, which should be critical in determining the direction of propagation, can be expected to decrease sharply with the number of molecules added since the Coulombic potential varies inversely with the distance of charge separation. This may account for the gradual decrease in the rate of the sequential addition of butadiene which was observed.

Acknowledgment. D.K.B. thanks the Natural Sciences and Engineering Research Council of Canada for the financial support of this research and the Canada Council for a Killam Research Fellowship.

Registry No. C_{60} fullerene dication, 120329-57-9; C_{70} fullerene dication, 133869-47-3; 1,3-butadiene, 106-99-0; C_{60} fullerene cation radical, 108739-25-9; C_{70} fullerene cation radical, 134932-61-9.

(8) Groenewold, G. S.; Gross, M. L. *J. Am. Chem. Soc.* **1984**, *106*, 6569.

A Mononuclear Nickel(II) Complex with $[NiN_3S_2]$ Chromophore That Readily Affords the Ni(I) and Ni(III) Analogues: Probe into the Redox Behavior of the Nickel Site in [FeNi] Hydrogenases

Narayan Baidya,[†] Marilyn M. Olmstead,[‡] and Pradip K. Mascharak*,[†]

Department of Chemistry and Biochemistry Thimann Laboratories, University of California Santa Cruz, California 95064
Department of Chemistry, University of California Davis, California 95616

Received July 9, 1992

Hydrogenases (H_2ase), the enzymes that catalyze the reversible oxidation of hydrogen,[1-5] are broadly divided into Fe-only and [FeNi] H_2ases, depending on their metal contents. Most of the [FeNi] H_2ases in their as-isolated forms display rhombic EPR signals (termed as Ni-A, g = 2.31, 2.23, 2.02, and Ni-B, g = 2.33, 2.16, 2.02).[1-3] Upon reduction, these signals disappear and further reduction affords a new rhombic signal (Ni-C, g = 2.19, 2.14, 2.02). These three signals (Ni-A, Ni-B, and Ni-C) are believed to be associated with the "unready", "ready", and "catalytically active" states of the enzymes, respectively. Several attempts have been made to establish the oxidation states of the nickel center at the active site of the enzyme during the catalytic cycle.[1,6-8] To date, two working mechanisms have been proposed on the basis of physicochemical studies. One mechanism supports the existence of Ni(III) in all three stages of the deactivation/activation processes.[1c,f,6] Quite in contrast, the other mechanism involves Ni(III) (Ni-A/Ni-B), Ni(II) (EPR silent), and Ni(I) (Ni-C) in the processes of H_2 utilization/evolution.[1e,2a,b,7,8] Rapid binding of H^- (substrate) and CO (an inhibitor) to the reduced form of the enzyme and the photoactivity of the substrate-bound species support this mechanism.[7]

In our synthetic analogue approach to the biological nickel site of [FeNi] H_2ase, we have isolated and structurally characterized

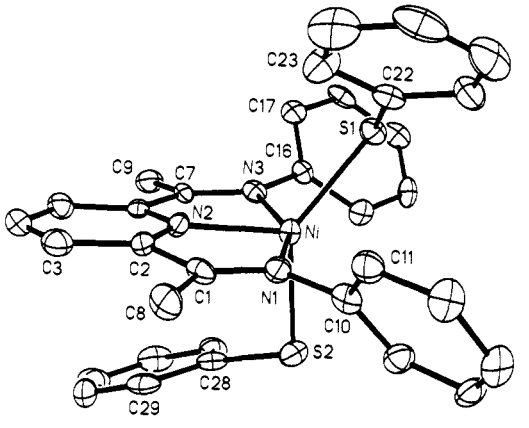

Figure 1. Thermal ellipsoid plot (50% probability level) of **1**. Hydrogen atoms are omitted for clarity. Selected bond distances (in Å): Ni–S(1), 2.263 (2); Ni–S(2), 2.351 (2); Ni–N(1), 2.110 (7); Ni–N(2), 1.936 (5); Ni–N(3), 2.131 (6); C(1)–N(1), 1.293 (9); N(3)–C(7), 1.317 (8); S(1)–C(22), 1.768 (8); N(1)–C(10), 1.431 (10). Selected bond angles (in deg): S(1)–Ni–S(2), 138.2 (1); N(1)–Ni–N(2), 78.3 (2); N(2)–Ni–N(3), 78.1 (2); N(1)–Ni–N(3), 156.4 (2); Ni–S(1)–C(22), 111.2 (2); Ni–S(2)–C(28), 105.3 (2); N(1)–Ni–S(2), 92.5 (1); S(1)–Ni–N(3), 90.5 (1); C(1)–C(2)–N(2), 114.6 (6).

0002-7863/92/1514-9666$03.00/0

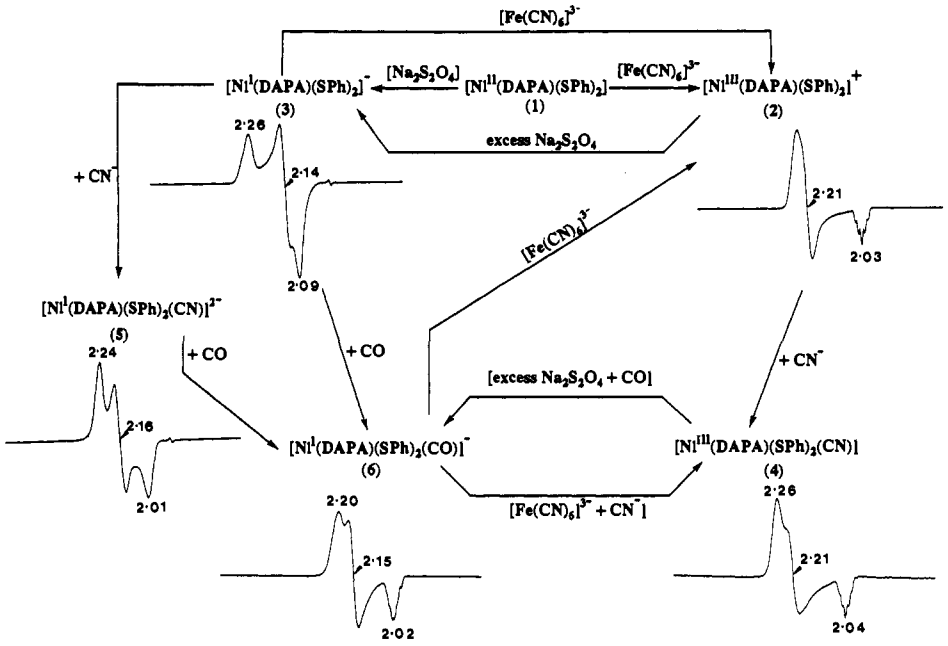

Figure 2. Schematic representation of the redox behavior of **1** along with the respective EPR spectra (100 K, DMF glass). Spectrometer setting: microwave frequency, 9.43 GHz; microwave power, 10 mW; modulation frequency, 100 kHz; modulation amplitude, 2G.

a set of analogues of the composition [Ni(terpy)(SR)$_2$] (terpy = 2,2′,2″-terpyridine, R = C_6F_5, 2,4,6-(*i*-Pr)$_3C_6H_2$, and 2,6-(Me)$_2C_6H_3$) that contain a trigonal bipyramidal (tbp) NiN_3S_2 chromophore.[9] X-ray absorption spectroscopic data for these analogues match well with those of the nickel site of the [FeNi] H_2ase from *Thiocapsa roseopersicina* (form C).[10] Though our model system is easily reduced to the Ni(I) species and binds both H^- and CO in the reduced form,[10a] oxidation of the nickel centers in this system appears difficult and proceeds to a small extent (g = 2.243, 2.199, and 2.049) and with significant decomposition. In our next attempt toward the synthesis of a better model system, we have selected another ligand, 2,6-bis[(1-phenylimino)ethyl]-pyridine (DAPA hereafter), that contains a less extensive π system and "harder" N donor centers. The synthesis, structure, and redox properties of [Ni(DAPA)(SPh)$_2$]CH_3CN (**1**) are reported in this account. Both oxidation and reduction of this model complex proceed readily with biologically relevant oxidants and reductants. The oxidized and reduced forms of **1** and their interactions with CO and CN^- have been studied by EPR spectroscopy, and the results are also included in this report.

The reaction of [Ni(DAPA)Cl_2][11] with 2.2 equiv of (Et_4N)(SPh) in acetonitrile generated a dark brown solution from which complex **1** was isolated as a reddish brown microcrystalline solid in 80% yield. Crystals for the X-ray work were obtained by slow cooling of the mother liquor. The structure[12] of **1** is shown in Figure 1. The coordination geometry around nickel is distorted tbp. The metric parameters of **1** are comparable to those observed with the terpy complexes.[9]

The redox behavior is **1** is schematically shown in Figure 2. Oxidation of **1** to [Ni^{III}(DAPA)(SPh)$_2$]$^+$ (**2**) is readily achieved in DMF (233–253 K) by (Et_4N)$_3$[Fe(CN)$_6$].[13] The single unpaired electron of the Ni(III) (d^7) center of **2** resides in the d_{z^2} orbital[14] ($g_\perp$ = 2.214, $g_\parallel$ = 2.032, $A_\parallel$ = 14.5 G). **2** is moderately stable at low temperature and amenable to binding studies. In contrast, the oxidized species from the analogous terpy complex [Ni(terpy)(2,6-(Me)$_2C_6H_3S)_2$] ($g_\perp$ = 2.243, $g_\parallel$ = 2.049, $A_\parallel$ = 16.5 G) is very unstable even at 233 K (Figure S1, supplementary material). Reduction of **1** in DMF by aqueous $Na_2S_2O_4$ generates the reduced species [Ni^I(DAPA)(SPh)$_2$]$^-$ (**3**), which exhibits a pseudorhombic EPR signal (g = 2.263, 2.138, 2.095) with the unpaired electron in the $d_{x^2-y^2}$ orbital.[14] The most important characteristic of these DAPA complexes is the reversibility observed in the transformation **2** ⇌ **3** (Figure 2).

Both **2** and **3** bind CN^- to afford the hexacoordinated cyanide adducts [Ni^{III}(DAPA)(SPh)$_2$(CN)] (**4**) (g = 2.263, 2.206, 2.043)

†University of California—Santa Cruz.
‡University of California—Davis.

(1) (a) Przybyla, A. E.; Robbins, J.; Menon, N.; Peck, H. D., Jr. *FEMS Microbiol. Rev.* **1992**, *88*, 109. (b) Moura, J. J. G.; Moura, I.; Teixeira, M.; Xavier, A. V.; Fauque, G. D.; LeGall, J. *Met. Ions Biol. Syst.* **1988**, *23*, 285. (c) Moura, J. J. G.; Teixeira, M.; Moura, I.; LeGall, J. In *The Bioinorganic Chemistry of Nickel*; Lancaster, J. R., Jr., Ed.; VCH Publishers: Deerfield Beach, FL, 1988; Chapter 9, p 191. (d) Bastian, N. R.; Wink, D. A.; Wackett, L. P.; Livingston, D. J.; Jordon, L. M.; Fox, J.; Orme-Johnson, W. H.; Walsh, C. T. In *The Bioinorganic Chemistry of Nickel*; Lancaster, J. R., Jr.; Ed.; VCH Publishers: Deerfield Beach, FL, 1988; Chapter 10, p 227. (e) Cammack, R.; Fernandez, V. M.; Schneider, K. In *The Bioinorganic Chemistry of Nickel*; Lancaster, J. R., Jr., Ed.; VCH Publishers: Deerfield Beach, FL, 1988; Chapter 8, p 167. (f) Moura, J. J. G.; Teixeira, M.; Moura, I.; Xavier, A. V.; LeGall, J. In *Frontiers of Bioinorganic Chemistry*; Xavier, A. V., Ed.; VCH Publishers: Deerfield Beach, FL, 1986; p 3.

(2) (a) Cammack, R. *Adv. Inorg. Chem.* **1988**, *32*, 297. (b) Albracht, S. P. J.; van der Zwaan, J. W.; Fontijn, R. D.; Slater, E. C. In *Frontiers of Bioinorganic Chemistry*; Xavier, A. V., Ed.; VCH Publishers: Deerfield Beach, FL, 1986; p 11. (c) Cammack, R.; Hall, D. O.; Rao, K. K. In *Gas Metabolism: Mechanistic, Metabolic and Biotechnological Aspects*; Poole, R. K., Dow, C. S., Eds.; Academic Press: New York, 1985.

(3) (a) Hausinger, R. P. *Microbiol. Rev.* **1987**, *51*, 22. (b) Walsh, C. T.; Orme-Johnson, W. H. *Biochemistry* **1987**, *26*, 4901.

(4) (a) Fauque, G.; Peck, H. D., Jr.; Moura, J. J. G.; Huynh, B. H.; Berlier, Y.; DerVartanian, D. V.; Teixeira, M.; Przybyla, A. E.; Lespinat, P. A.; Moura, I.; LeGall, J. *FEMS Microbiol. Rev.* **1988**, *54*, 299. (b) Vignais, P. M.; Colbeau, A.; Willison, J. C.; Jouranneau, Y. *Adv. Microb. Physiol.* **1985**, *26*, 155.

(5) (a) Moura, J. J. G.; Teixeira, M.; Moura, I. *J. Mol. Catal.* **1984**, *23*, 303. (b) Kondratieva, E. N.; Gogotov, I. N. *Adv. Biochem. Eng./Biotechnol.* **1983**, *28*, 139. (c) Adams, M. W. W.; Mortenson, L. E.; Chen, J.-S. *Biochim. Biophys. Acta* **1980**, *594*, 105.

(6) (a) Moura, J. J. G.; Teixeira, M.; Moura, I. *Pure Appl. Chem.* **1989**, *61*, 915. (b) Teixeira, M.; Moura, I.; Xavier, A. V.; Huynh, B.-H.; DerVartanian, D. V.; Peck, H. D., Jr.; LeGall, J.; Moura, J. J. G. *J. Biol. Chem.* **1985**, *260*, 8942.

(7) (a) van der Zwaan, J. W.; Coremans, J. M. C. C.; Bouwens, E. C. M.; Albracht, S. P. J. *Biochim. Biophys. Acta* **1990**, *1041*, 101. (b) Coremans, J. M. C. C.; van der Zwaan, J. W.; Albracht, S. P. J. *Biochim. Biophys. Acta* **1989**, *997*, 256. (c) van der Zwaan, J. W.; Albracht, S. P. J.; Fontijn, R. D.; Roelofs, Y. B. M. *Biochim. Biophys. Acta* **1986**, *872*, 208. (d) van der Zwaan, J. W.; Albracht, S. P. J.; Fontijn, R. D.; Slater, E. C. *FEBS Lett.* **1985**, *179*, 271.

and $[Ni^{I}(DAPA)(SPh)_2(CN)]^{2-}$ (**5**) (g = 2.235, 2.164, 2.013), respectively (Figure 2). The reduced species **3** also reacts with CO to produce the CO adduct $[Ni^{I}(DAPA)(SPh)_2(CO)]^{-}$ (**6**) (g = 2.198, 2.145, 2.023). Stepwise oxidation of **6** with $[Fe(CN)_6]^{3-}$ first generates an EPR-silent species and then the oxidized complex **2** (Figure S2, supplementary material). The coordinated CO in **6** therefore dissociates from the nickel center upon oxidation. This is also supported by the fact that no change in the EPR spectrum of **2** is observed under very high partial pressure of CO. It is interesting to note that CO replaces CN^- upon reduction of **4** in the presence of CO (the product being **6**), while CN^- recaptures the sixth coordination site upon oxidation (the product is **4**, Figure 2). Also, reaction of **5** with CO affords **6** as the sole product. It is thus clear that (a) CN^- binds to both the oxidized and the reduced species (**2** and **3**), (b) CO binds only to the reduced species, and (c) CO binds to the reduced species more strongly than CN^-.

In conclusion, complex **1** is the first example of a model system for the nickel site of the [FeNi] H_2ases that could be readily oxidized and reduced to the corresponding Ni(III) and Ni(I) species. Binding studies with these species reveal that the EPR spectra of the pentacoordinated complexes (be it oxidized or reduced) are mostly axial while the hexacoordinated species exhibit more rhombic EPR signals. The same trend has been observed with the terpy system. It is therefore not unreasonable to assume the presence of hexacoordinated nickel centers in both the oxidized (Ni-A/Ni-B) and reduced (Ni-C) forms of the enzyme. Since the combined presence of aromatic heterocyclic nitrogens and thiolato sulfurs in the first coordination sphere of nickel in **1** provides stabilization to three oxidation states (+3, +2, and +1), it is quite likely that ligation of imidazole nitrogens and cysteinyl sulfurs creates a similar electronic environment around the biological nickel site, which in turn allows it to assume the same three oxidation states during turnover.

Acknowledgment. Financial support from the donors of the Petroleum Research Fund, administered by the American Chemical Society, is gratefully acknowledged.

Supplementary Material Available: EPR spectrum of $[Ni^{III}(terpy)(2,6\text{-}(Me)_2C_6H_3S)_2]^+$ (Figure S1), EPR titration (stepwise oxidation) of **6** with $[Fe(CN)_6]^{3-}$ (Figure S2), crystal structure data for **1** including tables of atomic coordinates (Table S1), complete bond distances (Table S2) and angles (Table S3), anisotropic thermal parameters (Table S4), and H-atom coordinates (Table S5) (14 pages); table of observed and calculated structure factors (Table S6) (39 pages). Ordering information is given on any current masthead page.

(8) Cammack, R.; Fernandez, V. M.; Schneider, K. *Biochimie* **1986**, *68*, 85. (b) Fernandez, V. M.; Hatchikian, E. C.; Patil, D. S.; Cammack, R. *Biochim. Biophys. Acta* **1986**, *883*, 145.

(9) Baidya, N.; Olmstead, M. M.; Mascharak, P. K. *Inorg. Chem.* **1991**, *30*, 929.

(10) (a) Baidya, N.; Olmstead, M. M.; Whitehead, J. P.; Bagyinka, C.; Maroney, M. J.; Mascharak, P. K. *Inorg. Chem.* **1992**, *31*, 3612. (b) Maroney, M. J.; Colpas, G. J.; Bagyinka, C.; Baidya, N.; Mascharak, P. K. *J. Am. Chem. Soc.* **1991**, *113*, 3962. (c) Colpas, G. J.; Maroney, M. J.; Bagyinka, C.; Kumar, M.; Willis, W. S.; Suib, S. L.; Baidya, N.; Mascharak, P. K. *Inorg. Chem.* **1991**, *30*, 920.

(11) Alyea, E. C.; Ferguson, G.; Restivo, R. J. *Inorg. Chem.* **1975**, *14*, 2491.

(12) X-ray analysis: red-brown plates from acetonitrile, $NiC_{35}H_{32}N_4S_2$ (**1**), monoclinic space group $P2_1/c$, a = 23.012 (7) Å, b = 17.814 (5) Å, c = 15.698 (4) Å, β = 108.52 (2)°, V = 6099 (5) Å^3, Z = 8, d_{calcd} = 1.375 g/cm^3, R = 6.46%, R_w = 5.40%. The structure was solved by direct methods (SHELXTL PLUS, version 4.2).

(13) Mascharak, P. K. *Inorg. Chem.* **1986**, *25*, 245.

(14) Salerno, J. In *The Bioinorganic Chemistry of Nickel*; Lancaster, J. R., Jr., Ed.; VCH Publishers: Deerfield Beach, FL, 1988; Chapter 3, p 53.

Synthesis of $[Me_2SCu(C_6H_2\text{-}2,4,6\text{-}t\text{-}Bu_3)]$ and $[(Me_2S)_2Cu(\mu\text{-}C_6H_2\text{-}2,4,6\text{-}Ph_3)Cu(C_6H_2\text{-}2,4,6\text{-}Ph_3)]$: Mononuclear and Dinuclear Organocopper(I) Species of Formula $[CuR\cdot Solvate]_{1 \text{ or } 2}$

Xiaoming He, Marilyn M. Olmstead, and Philip P. Power*

Department of Chemistry
University of California
Davis, California 95616

Received July 24, 1992

The solid- and solution-phase structures of organocopper compounds are a topic of considerable current interest.[1,2] Part of the reason for this is the extreme importance of these compounds, in particular their ionic derivatives (organocuprates), for organic synthesis.[3] In addition, their structures are inherently interesting not least because of their isovalent relationship to organolithium compounds.[4] Owing to their similar sizes, it is often possible to interchange Li for Cu in related aggregates while preserving the overall integrity of the molecules themselves. An illustration of this phenomenon is provided by the series of compounds $Cu_4Ph_4(SMe_2)_2$, $Li_2Cu_2Ph_4(SMe_2)_3$, and $Li_4Ph_4(SMe_2)_4$, which contain different Li:Cu ratios but remain tetrametallic species.[5] These complexes are not isostructural, however, owing to the preference of a σ-bonded, two-coordinate Cu^+ ion for linear or near linear coordination. This restriction, in contrast to the coordinative flexibility of Li^+, exerts a profound influence on the structure of organocopper compounds.[4] One consequence is that organocopper structures having simple monodentate groups and lower aggregation numbers than four are practically unknown, whereas they are quite common in the case of lithium compounds. This may be understood in part by assuming that the preference for linear coordination at Cu imposes increasingly acute angles at the organo group as illustrated schematically by

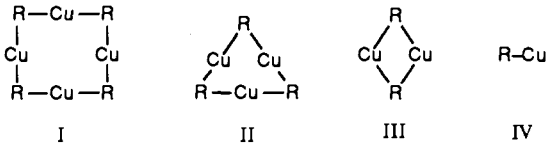

I II III IV

Structures related to type II, in which the angle at R is ideally 60°, have not been reported for a purely organometallic species,[6] and only one representative of the species IV featuring a one-coordinate unsolvated copper has been published.[7] No compounds corresponding to the formula $(CuR)_2$, where R is a monodentate ligand, have yet appeared.[8] In this paper, the first examples of

(1) van Koten, G. *J. Organomet. Chem.* **1990**, *400*, 283.

(2) Power, P. P. *Prog. Inorg. Chem.* **1991**, *39*, 75.

(3) Posner, G. H. *An Introduction to Synthesis Using Organocopper Reagents*; Wiley: New York, 1980. van Koten, G.; Noltes, J. G. *Comprehensive Organometallic Chemistry*; Wilkinson, G., Stone, F. G. A., Abel, E. W., Eds. Pergamon: Oxford, 1984.

(4) Setzer, W. N.; Schleyer, P. v. R. *Adv. Organomet. Chem.* **1985**, *24*, 353.

(5) Olmstead, M. M.; Power, P. P. *J. Am. Chem. Soc.* **1990**, *112*, 8008. A further example of this type of relationship is seen with use of the chelating ligand $C_6H_4\text{-}2\text{-}CH_2NMe_2$.[1]

(6) Some related species that have been reported are the thiolate $[Cu\{SC_6H_4\text{-}2\text{-}CHMeNMe_2\}]_3$ (Knotter, D. M.; van Koten, G.; van Maanen, H. L.; Grove, D. M.; Spek, A. L. *Angew. Chem., Int. Ed. Engl.* **1989**, *28*, 341), the species $[Cu_3(\mu\text{-}C_6H_2Me_3)(\mu\text{-}O_2CPh)_2]$ (Aalten, H. L.; van Koten, G.; Goubitz, K.; Stam, C. H. *Organometallics* **1989**, *8*, 2293), and the amide $[Cu\{N(SiMePh_2)_2\}]_3$ (Chen, H.; Olmstead, M. M.; Shoner, S. C.; Power, P. P. *J. Chem. Soc., Dalton Trans.* **1992**, 451). For further examples, see ref 1.

(7) Lingnau, R.; Strähle, J. *Angew. Chem., Int. Ed. Engl.* **1988**, *27*, 436.

(8) Dimeric organocopper species are known in the case of chelating ligands such as $CH(SiMe_3)$(2-pyridine). These compounds, however, contain no multicenter bonding. The dimeric formula is a consequence of the chelating effect of the ligand, which allows an almost linear geometry at the coppers and imposes a short Cu···Cu interaction, 2.412 (1) Å: Papasergio, R. I.; Raston, C. L.; White, A. L. *J. Chem. Soc., Chem. Commun.* **1983**, 1419.

0002-7863/92/1514-9668$03.00/0